

预测纳米纤维复合材料有效弹性性能的界面模型和界面相模型

崔春丽, 徐耀玲

The Interface Model and the Interphase Model for Predicting the Effective Elastic Properties of Nano-Fiber Composites

CUI Chunli and XU Yaoling

在线阅读 View online: <https://doi.org/10.21656/1000-0887.420231>

您可能感兴趣的其他文章

Articles you may be interested in

横观各向同性基体复合材料的等效弹性常数

Effective Elastic Properties of Transversely Isotropic Matrix Based Composites

应用数学和力学. 2018, 39(7): 750-765 <https://doi.org/10.21656/1000-0887.380267>

基于特征正交分解的材料微结构参数化表征模型及等效性能优化设计

A POD-Based Parameterization Model for Material Microstructure Representation and Its Application to Optimal Design of Material Effective Mechanical Properties

应用数学和力学. 2017, 38(7): 727-742 <https://doi.org/10.21656/1000-0887.370279>

层状弹性材料界面J积分的产生和特征

Characteristics and Generation of Interface J integrals in Layered Elastic Materials

应用数学和力学. 2017, 38(10): 1155-1165 <https://doi.org/10.21656/1000-0887.370270>

新型轻质复合材料夹芯结构振动阻尼性能研究进展

Progresses in the Study on Vibration Damping Properties of Novel Lightweight Composite Sandwich Structures

应用数学和力学. 2017, 38(4): 369-398 <https://doi.org/10.21656/1000-0887.370328>

构成单材料裂纹和双材料界面裂纹有限应力集中的一般解析函数

Construction of General Analytic Functions With Finite Stress Concentration for Mono-Material Cracks and Bi-Material Interface Cracks

应用数学和力学. 2018, 39(12): 1364-1376 <https://doi.org/10.21656/1000-0887.390030>

小波神经网络模型预测二氧化碳+水溶液体系界面张力

Prediction of Interfacial Tension Between CO₂ and Brine With the Wavelet Neural Network Method

应用数学和力学. 2017, 38(10): 1136-1145 <https://doi.org/10.21656/1000-0887.370339>



关注微信公众号, 获得更多资讯信息

预测纳米纤维复合材料有效弹性性能的 界面模型和界面相模型*

崔春丽, 徐耀玲

(燕山大学 河北省重型装备与大型结构力学可靠性重点实验室, 河北 秦皇岛 066004)

摘要: 基于广义自洽法, 同时采用 Gurtin-Murdoch 界面模型和界面相模型研究了纳米纤维复合材料的有效弹性性能, 获得了两种模型下有效体积模量的封闭解析解和计算有效面内剪切模量数值解的全部公式. 基于界面模型的解答, 讨论了有效体积模量和有效面内剪切模量的界面效应. 证明了界面模型的解答可由界面相模型的解答退化得到, 其中有效体积模量可以实现解析退化, 有效面内剪切模量则可以数值退化. 以含纳米孔洞的金属铝为例, 比较了两种模型计算结果的差异. 结果表明, 当纳米孔洞半径较小时, 两个模型的结果存在很大差异, 而当半径较大时两个模型的结果差别不大.

关键词: 纳米纤维复合材料; 有效弹性性能; 界面模型; 界面相模型

中图分类号: O31 **文献标志码:** A **DOI:** 10.21656/1000-0887.420231

The Interface Model and the Interphase Model for Predicting the Effective Elastic Properties of Nano-Fiber Composites

CUI Chunli, XU Yaoling

(Key Laboratory of Mechanical Reliability for Heavy Equipments and Large Structures of Hebei Province, Yanshan University, Qinhuangdao, Hebei 066004, P.R.China)

Abstract: The effective bulk modulus and the effective in-plane shear modulus of nano-fiber composites were investigated with the interface model and the interphase model based on the generalized self-consistent method, and the closed-form analytical solutions of the effective bulk modulus and all equations for numerically predicting effective in-plane shear modulus based on the 2 models, were presented. With the interface model, interface effects of the effective bulk modulus and the effective in-plane shear modulus were discussed through numerical examples. Furthermore, the solutions of the interface model were proved to be degenerated ones of those of the interphase model, where the effective bulk modulus can be obtained through analytical degeneration and the numerical results of the effective in-plane shear modulus through numerical degeneration. An example of aluminium containing nano voids shows that, the effective bulk modulus and the effective in-plane shear modulus predicted with the interface model have large deviations from those with the interphase model for small void radii, however, small deviations for larger void radii.

Key words: nano-fiber composite; effective elastic property; interface model; interphase model

* 收稿日期: 2021-08-05; 修订日期: 2021-11-24

作者简介: 崔春丽(1995—), 女, 硕士生(E-mail: cuichunli@stumail.yzu.edu.cn);
徐耀玲(1968—), 男, 教授(通讯作者. E-mail: xylysu@163.com).

引用格式: 崔春丽, 徐耀玲. 预测纳米纤维复合材料有效弹性性能的界面模型和界面相模型[J]. 应用数学和力学, 2022, 43(8): 877-887.

引言

由于具有多方面优异的性能,纳米复合材料在众多领域获得了越来越广泛的应用^[1-2].界面效应对纳米复合材料的力学性能有着显著影响^[3-4],近年来一直受到众多学者的关注.Gurtin-Murdoch 界面模型^[5-6]和界面相模型^[7-8]是研究纳米夹杂问题的两种模型,广泛用于含纳米夹杂材料的应力场和纳米复合材料宏观有效性能的研究.

在 Gurtin-Murdoch 界面模型中,夹杂与基体间的界面无厚度但有其自身的力学性质和本构关系,跨越该界面应力不连续.利用 Gurtin-Murdoch 界面模型, Luo 等^[9]给出了无限介质中单个椭圆柱形纳米夹杂反平面问题的解析解; Tian 等^[10-11]获得了无限介质中单个圆形和椭圆形纳米夹杂平面问题的解答并对应力场进行了细致的分析; Dong 等^[12]给出了包含任意形状纳米夹杂的有限区域平面问题应力场的边界元求解方法; Mogilevskaya 等^[13]讨论了无限介质中多纳米夹杂之间的相互作用.基于细观力学方法(复合球集模型、Mori-Tanaka 法和广义自洽法), Duan 等^[14]预测了含纳米球形孔洞材料的有效体积模量和剪切模量,并对尺度效应进行了讨论.Chen 等^[15]预测了含球形纳米夹杂复合材料的有效热力学性质,建立了有效体积模量和有效热膨胀系数之间的精确关联.肖俊华等^[16]利用广义自洽法获得了纳米涂层纤维复合材料有效反平面剪切模量的解析解,并算例分析了涂层刚度和厚度对有效反平面剪切模量的影响.

对于实际的复合材料系统,两材料相之间存在着一定厚度的界面相,将界面视为无厚度的界面模型仅为实际情况的一种简化,从这个意义上讲,界面相模型更为合理.近年来,界面相模型受到越来越多学者的关注.利用界面相模型, Odegard 等^[7]预测了四种不同界面处理方式时,纳米硅颗粒/聚乙烯胺复合材料的有效弹性模量,算例中界面相性质和厚度由分子动力学模拟得到.Li 等^[17]预测了含有三种典型纳米夹杂(球形、短纤维形和圆盘形)复合材料的有效弹性性质,讨论了夹杂的尺度和形状效应.Paliwal 等^[18]用广义自洽法研究了含纳米球形孔洞材料的有效弹性常数,并用算例给出了有效体积模量和剪切模量随孔洞半径和孔洞体积分数的变化.Wang 等^[19-20]研究了球形和圆柱形纳米夹杂复合材料的有效弹性性质.

界面模型和界面相模型同为研究纳米夹杂问题的模型,两者之间联系受到了学者们的关注.Benveniste 等^[21]的研究表明,通过合适选择界面相的弹性性质和厚度,界面相模型可以模拟 Gurtin-Murdoch 界面模型.Wang 等^[22]给出了界面相性质与界面性质之间的关系,以纳米颗粒复合材料的应力为例,讨论了界面相模型模拟界面模型的问题.Mogilevskaya 等^[13]以二维纳米夹杂的应力为例讨论了界面相模型模拟界面模型的问题,文献中采用的界面相性质与界面性质之间的关系与 Wang 等^[22]的相同.至于两个模型结果之间的差异,据笔者所知,目前的研究还很少见.

基于广义自洽法,本文推导了两种模型下预测纳米纤维复合材料有效体积模量的封闭解析解和有效面内剪切模量数值解的全部公式.在界面相 Poisson 比取为零的情况下,将文献 [22] 中的界面相性质与界面性质之间的关系式表述为更加简洁的形式,讨论了界面相模型模拟界面模型的问题.以含纳米孔洞的金属铝为例,展示了界面模型与界面相模型计算结果的差异.

1 两种模型和基本方程

基于广义自洽法的两种模型如图 1 所示,其中图 1(a) 为界面模型,图 1(b) 为界面相模型.在图 1(a) 中,分别用 Ω_f , Ω_m 和 Ω_{em} 表示纤维、基体和等效介质(此处及以后,角标 f, m 和 em 分别表示纤维、基体和等效介质); S_f 为纤维与基体间的界面,无厚度但有其自身的力学性质和本构关系,跨越该界面应力不连续(非经典界面条件); S_m 为基体与等效介质间的经典界面,在该界面上应力连续;两个界面的半径分别为 R_f 和 R_m .在图 1(b) 中,分别用 Ω_1 , Ω_3 和 Ω_4 表示纤维、基体和等效介质, Ω_2 为纤维与基体之间的界面相;在讨论两个模型之间关联时被用来模拟界面模型中的零厚度界面 S_f , $S_i(i=1, 2, 3)$ 为各材料相之间的经典界面; $R_i(i=1, 2, 3)$ 为各界面的半径.在纤维中心处建立直角坐标系 xOy 和极坐标系 $rO\theta$, 远场作用均匀应力为 σ_x^∞ , σ_y^∞ 和 τ_{xy}^∞ .

根据弹性理论的复变函数方法,平面问题的弹性场可由两个解析函数(应力函数) $\phi(z)$ 和 $\psi(z)$ 描述^[23]:

$$2\mu(u + iv) = \kappa\phi(z) - \overline{z\phi'(z)} - \overline{\psi(z)}, \quad (1)$$

$$\sigma_x + \sigma_y = 2[\phi'(z) + \overline{\phi'(z)}], \tag{2}$$

$$\sigma_y - \sigma_x + 2i\tau_{xy} = 2[\bar{z}\phi''(z) + \psi'(z)], \tag{3}$$

$$X_1 + iX_2 = -i[\phi(z) + \overline{z\phi'(z)} + \overline{\psi(z)}], \tag{4}$$

式中, u, v 为位移分量; $\sigma_x, \sigma_y, \tau_{xy}$ 为应力分量; $X_1 + iX_2$ 为任意弧段上的合力; μ 为剪切模量; 复变量 $z = x + iy$. 对平面应变问题, $\kappa = 3 - 4\nu$, ν 为 Poisson 比.

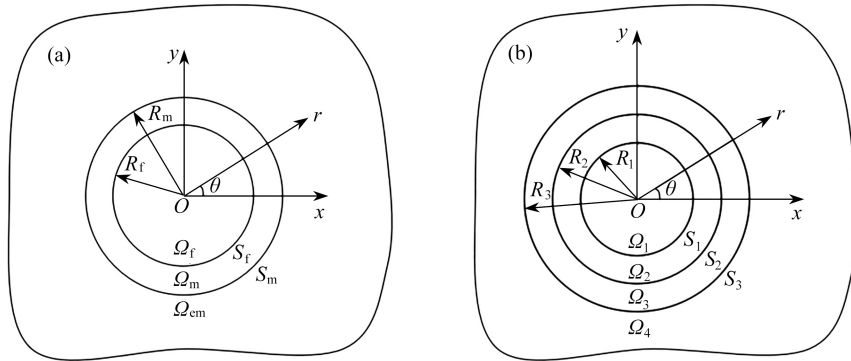


图 1 预测纳米纤维复合材料有效性质的两种模型: (a) 界面模型; (b) 界面相模型

Fig. 1 Two models for predicting the effective elastic properties of nano-fiber composites: (a) the interface model; (b) the interphase model

在极坐标系中

$$\sigma_r + \sigma_\theta = 2[\phi'(z) + \overline{\phi'(z)}], \tag{5}$$

$$\sigma_\theta - \sigma_r + 2i\tau_{r\theta} = 2[\bar{z}\phi''(z) + \psi'(z)]e^{2i\theta}, \tag{6}$$

$$\varepsilon_\theta + \varepsilon_r = \frac{1}{\Gamma}[\varphi'(z) + \overline{\varphi'(z)}], \tag{7}$$

$$\varepsilon_\theta - \varepsilon_r + 2i\varepsilon_{r\theta} = \frac{1}{\mu}[\bar{z}\phi''(z) + \psi'(z)]e^{2i\theta}, \tag{8}$$

式中, $\sigma_r, \sigma_\theta, \tau_{r\theta}$ 和 $\varepsilon_r, \varepsilon_\theta, \varepsilon_{r\theta}$ 分别为极坐标系中的应力和应变分量; $\Gamma = \lambda + \mu, \lambda = E\nu/((1 + \nu)(1 - 2\nu))$ 为 Lamé 系数.

由式 (5) ~ (8) 可得

$$\sigma_r - i\tau_{r\theta} = [\phi'(z) + \overline{\phi'(z)}] - [\bar{z}\phi''(z) + \psi'(z)]e^{2i\theta}, \tag{9}$$

$$\varepsilon_\theta = \frac{1}{2\Gamma}[\phi'(z) + \overline{\phi'(z)}] + \frac{1}{4\mu}[\bar{z}\phi''(z) + \psi'(z)]e^{2i\theta} + \frac{1}{4\mu}[\overline{z\phi''(z)} + \overline{\psi'(z)}]e^{-2i\theta}. \tag{10}$$

2 有效体积模量和有效面内剪切模量

2.1 界面模型

在图 1(a) 纤维、基体和等效介质区域, 将应力函数分别展开成 Taylor 级数和 Laurent 级数:

$$\varphi_f(z) = \sum_{k=1}^{\infty} a_k^f z^k, \quad \psi_f(z) = \sum_{k=1}^{\infty} b_k^f z^{-k}, \quad z \in \Omega_f, \tag{11}$$

$$\phi_m(z) = \sum_{k=1}^{\infty} (a_k^m z^k + a_{-k}^m z^{-k}), \quad \psi_m(z) = \sum_{k=1}^{\infty} (b_k^m z^k + b_{-k}^m z^{-k}), \quad z \in \Omega_m, \tag{12}$$

$$\phi_{em}(z) = \sum_{k=1}^{\infty} (a_k^{em} z^k + a_{-k}^{em} z^{-k}), \quad \psi_{em}(z) = \sum_{k=1}^{\infty} (b_k^{em} z^k + b_{-k}^{em} z^{-k}), \quad z \in \Omega_{em}. \tag{13}$$

将式 (13) 代入式 (2) 和 (3), 并利用无穷远应力条件:

$$(\sigma_x + \sigma_y)_{z \rightarrow \infty} = \sigma_x^\infty + \sigma_y^\infty, (\sigma_x - \sigma_y + 2i\tau_{xy})_{z \rightarrow \infty} = \sigma_y^\infty - \sigma_x^\infty + 2i\tau_{xy}^\infty, \quad (14)$$

可得应力函数 $\phi_{em}(z)$ 和 $\psi_{em}(z)$ 级数展开式中的正幂项系数只有 a_1^{em} 和 b_1^{em} 不为零,且

$$a_1^{em} = \frac{1}{4}(\sigma_x^\infty + \sigma_y^\infty), b_1^{em} = \frac{1}{2}(\sigma_y^\infty - \sigma_x^\infty + 2i\tau_{xy}^\infty). \quad (15)$$

界面 S_f 的本构关系为^[24-25]

$$\sigma_\theta^{S_f} = (2\mu^{S_f} + \lambda^{S_f})\varepsilon_\theta^{S_f} = E^{S_f}\varepsilon_\theta^{S_f}, \quad (16)$$

式中, $\sigma_\theta^{S_f}$ 和 $\varepsilon_\theta^{S_f}$ 为界面环向应力和应变, μ^{S_f} 和 λ^{S_f} 为界面 Lamé系数.

界面 S_f 上的位移连续、应力跳跃条件可表示为

$$\begin{cases} (u_f + iv_f)_{z \in S_f} = (u_m + iv_m)_{z \in S_f}, \\ (\sigma_r^m - i\tau_{r\theta}^m)_{z \in S_f} - (\sigma_r^f - i\tau_{r\theta}^f)_{z \in S_f} = \frac{1}{R_f} \left(\sigma_\theta^{S_f} + i \frac{\partial \sigma_\theta^{S_f}}{\partial \theta} \right), \end{cases} \quad (17)$$

界面应变与相邻材料环向应变相等,即 $\varepsilon_\theta^{S_f} = \varepsilon_\theta^f = \varepsilon_\theta^m$,在下面推导中取 $\varepsilon_\theta^{S_f} = \varepsilon_\theta^m$.

界面 S_m 上的位移和应力满足连续条件:

$$\begin{cases} (u + iv)_m = (u + iv)_{em}, \\ (X_1 + iX_2)_m = (X_1 + iX_2)_{em}. \end{cases} \quad (18)$$

利用式(1)、(4)、(9)和(10),由界面条件式(17)和(18)可推得级数展开式(11)~(13)中除由远场应力条件确定的系数 a_1^{em} 和 b_1^{em} 外,还有12个系数($a_1^f, a_3^f, b_1^f, a_1^m, a_{-1}^m, a_3^m, b_1^m, b_{-1}^m, b_{-3}^m, a_{-1}^{em}, b_{-1}^{em}, b_{-3}^{em}$)不为零.这些系数与未知的等效介质的力学参数相关,由附录A中的12个方程确定.

跨越界面 S_f 位移连续、应力跳跃,此时代表体单元内 $\Omega_f + \Omega_m$ 的平均应变和平均应力为^[15,21]

$$\begin{cases} \bar{\varepsilon}_{ij} = c_f \bar{\varepsilon}_{ij}^f + c_m \bar{\varepsilon}_{ij}^m, \\ \bar{\sigma}_{ij} = c_f \bar{\sigma}_{ij}^f + c_m \bar{\sigma}_{ij}^m - \frac{c_f}{V_f} \int_S (\sigma_{ir}^f - \sigma_{ir}^m) n_r x_j dS, \end{cases} \quad (19)$$

式中, $c_f = R_f^2/R_m^2$ 和 $c_m = (1 - c_f)$ 分别为纤维和基体的体积分; V_f 为纤维体积;角标 $i, j, r = x, y, n_x = \cos \theta$ 和 $n_y = \sin \theta$ 为 S_f 单位外法向量在 x 轴和 y 轴方向上的投影.积分在界面 S_f 上进行, $x_x = R_f \cos \theta, x_y = R_f \sin \theta$.

为确定有效体积模量,施加远场条件 $\sigma_x^\infty = \sigma_y^\infty \neq 0, \tau_{xy}^\infty = 0$.由式(19)可推得平均应力 $\bar{\sigma}_x + \bar{\sigma}_y$ 和平均应变 $\bar{\varepsilon}_x + \bar{\varepsilon}_y$ 只与上述14个系数中的 a_1^f, a_1^m 和 b_{-1}^m 显式相关.而由式(A1)和(A2), a_1^m 和 b_{-1}^m 又可由 a_1^f 表示,进而 $\bar{\sigma}_x + \bar{\sigma}_y$ 和 $\bar{\varepsilon}_x + \bar{\varepsilon}_y$ 可由 a_1^f 表示如下:

$$\bar{\sigma}_x + \bar{\sigma}_y = 4[c_f + (1 - c_f)M_1 + M_1 C_3 c_f - M_{-1} C_4 c_f / R_f^2] a_1^f, \quad (20)$$

$$\bar{\varepsilon}_x + \bar{\varepsilon}_y = 2[c_f / \Gamma_f + M_1 (1 - c_f) / \Gamma_m] a_1^f, \quad (21)$$

其中

$$\begin{cases} M_1 = \frac{(2C_4 + 1)(\kappa_f - 1) + 2C_1}{C_1(\kappa_m + 1)}, \\ M_{-1} = \frac{2R_f^2[(C_3 - 1)(\kappa_f - 1) + C_1(\kappa_m - 1)]}{C_1(\kappa_m + 1)}, \end{cases} \quad (22)$$

式中 C_1, C_3 和 C_4 的定义见附录A.

由式(20)和(21),可得有效体积模量 B_{em} 的封闭解析解:

$$B_{em} = \frac{\bar{\sigma}_x + \bar{\sigma}_y}{2(\bar{\varepsilon}_x + \bar{\varepsilon}_y)} = \frac{c_f + (1 - c_f)M_1 + M_1 C_3 c_f - M_{-1} C_4 c_f / R_f^2}{c_f / \Gamma_f + M_1 (1 - c_f) / \Gamma_m}. \quad (23)$$

确定有效面内剪切模量时施加远场条件 $\sigma_x^\infty = \sigma_y^\infty = 0, \tau_{xy}^\infty \neq 0$.由式(19)计算得代表性体积单元内 $\Omega_f + \Omega_m$ 的平均切应力 $\bar{\sigma}_{xy}$ 和切应变 $\bar{\varepsilon}_{xy}$ 分别为

$$\bar{\sigma}_{xy} = Q_1 + Q_2 + Q_3, \tag{24}$$

$$\bar{\varepsilon}_{xy} = c_f(3a_3^f R_f^2 + b_1^f)/(2\mu_f) + (1 - c_f)[3a_3^m(R_m^2 + R_f^2) + b_1^m]/(2\mu_m), \tag{25}$$

式中

$$\begin{cases} Q_1 = c_f(3a_3^f R_f^2 + b_1^f) + (1 - c_f)[3a_3^m(R_m^2 + R_f^2) + b_1^m], \\ Q_2 = c_f C_3(3a_3^m R_f^2 + a_{-1}^m/R_f^2), \\ Q_3 = c_f C_4(6a_3^m R_f^2 - 2a_{-1}^m/R_f^2 + b_1^m + 3b_{-3}^m/R_f^4). \end{cases} \tag{26}$$

有效面内剪切模量 μ_{em} 为

$$\mu_{em} = \frac{\bar{\sigma}_{xy}}{2\bar{\varepsilon}_{xy}} = \frac{Q_1 + Q_2 + Q_3}{c_f(3a_3^f R_f^2 + b_1^f)/\mu_f + (1 - c_f)[3a_3^m(R_m^2 + R_f^2) + b_1^m]/\mu_m}. \tag{27}$$

上式为一个隐式表达式, 在由式 (23) 求出体积模量后, 需联立方程 (A5) ~ (A12) 数值求解才能确定 μ_{em} .

2.2 界面相模型

在图 1(b) 各区域将应力函数分别展开成 Taylor 级数和 Laurent 级数:

$$\phi_1(z) = \sum_{k=1}^{\infty} a_k^{(1)} z^k, \quad \psi_1(z) = \sum_{k=1}^{\infty} b_k^{(1)} z^k, \quad z \in \Omega_1, \tag{28}$$

$$\phi_i(z) = \sum_{k=1}^{\infty} (a_k^{(i)} z^k + a_{-k}^{(i)} z^{-k}), \quad \psi_i(z) = \sum_{k=1}^{\infty} (b_k^{(i)} z^k + b_{-k}^{(i)} z^{-k}), \quad z \in \Omega_i, \quad i = 2, 3, 4. \tag{29}$$

由远场应力条件式 (14), 亦可知应力函数 $\phi_4(z)$ 和 $\psi_4(z)$ 级数展开式中的正幂项系数只有 $a_1^{(4)}$ 和 $b_1^{(4)}$ 不为零,

$$a_1^{(4)} = (\sigma_x^\infty + \sigma_y^\infty)/4, \quad b_1^{(4)} = (\sigma_y^\infty - \sigma_x^\infty + 2i\tau_{xy}^\infty)/2. \tag{30}$$

在各相界面 $S_i (i=1, 2, 3)$ 上, 位移和应力连续条件表示为

$$\begin{cases} (u + iv)_i = (u + iv)_{i+1}, \\ (X_1 + iX_2)_i = (X_1 + iX_2)_{i+1}, \end{cases} \quad i = 1, 2, 3, \tag{31}$$

式中, 下标 i 表示括号内的函数从区域 Ω_i 趋于边界 S_i 取值.

由界面条件式 (31), 通过分析可推得级数展开式 (28)、(29) 中除由远场条件确定的 $a_1^{(4)}$ 和 $b_1^{(4)}$ 外, 还有 18 个不为零系数 ($a_1^{(1)}, a_3^{(1)}, b_1^{(1)}, a_1^{(2)}, a_{-1}^{(2)}, a_3^{(2)}, b_1^{(2)}, b_{-1}^{(2)}, b_{-3}^{(2)}, a_1^{(3)}, a_{-1}^{(3)}, a_3^{(3)}, b_1^{(3)}, b_{-1}^{(3)}, b_{-3}^{(3)}, a_{-1}^{(4)}, b_{-1}^{(4)}, b_{-3}^{(4)}$). 这些系数与未知的等效介质的力学参数相关, 可由附录 B 中的 6 组共 18 个方程确定.

施加远场条件 $\sigma_x^\infty = \sigma_y^\infty \neq 0, \tau_{xy}^\infty = 0$, 由式 (19) 可推得平均应力 $\bar{\sigma}_x + \bar{\sigma}_y$ 和平均应变 $\bar{\varepsilon}_x + \bar{\varepsilon}_y$ 只与上述 20 个系数中的 $a_1^{(1)}, a_1^{(2)}$ 和 $a_1^{(3)}$ 显式相关. 由式 (B1) 和 (B2), $a_1^{(2)}$ 和 $a_1^{(3)}$ 又可由 $a_1^{(1)}$ 表示, 进而 $\bar{\sigma}_x + \bar{\sigma}_y$ 和 $\bar{\varepsilon}_x + \bar{\varepsilon}_y$ 可由 $a_1^{(1)}$ 表示如下:

$$\bar{\sigma}_x + \bar{\sigma}_y = 4[c_1 + L_1 c_2 + L_2(1 - c_1 - c_2)]a_1^{(1)}, \tag{32}$$

$$\bar{\varepsilon}_x + \bar{\varepsilon}_y = 2[c_1/\Gamma_1 + L_1 c_2/\Gamma_2 + L_2(1 - c_1 - c_2)/\Gamma_3]a_1^{(1)}, \tag{33}$$

式中, c_1 和 c_2 分别为纤维和界面相的体积分, $c_1 = R_1^2/R_3^2, c_2 = (R_2^2 - R_1^2)/R_3^2$;

$$\begin{cases} L_1 = \frac{2g_{12} + \kappa_1 - 1}{g_{12}(\kappa_2 + 1)}, \\ L_2 = \frac{(2g_{23} + \kappa_2 - 1)(2g_{12} + \kappa_1 - 1) + 2(R_1/R_2)^2(g_{23} - 1)[g_{12}(\kappa_2 - 1) - \kappa_1 + 1]}{g_{12}g_{23}(\kappa_2 + 1)(\kappa_3 + 1)}, \end{cases} \tag{34}$$

式中, g_{12} 和 g_{23} 的定义见附录 B.

由式 (32) 和 (33), 可得有效体积模量 B_4 的封闭解析解:

$$B_4 = \frac{\bar{\sigma}_x + \bar{\sigma}_y}{2(\bar{\varepsilon}_x + \bar{\varepsilon}_y)} = \frac{c_1 + L_1 c_2 + L_2(1 - c_1 - c_2)}{c_1/\Gamma_1 + L_1 c_2/\Gamma_2 + L_2(1 - c_1 - c_2)/\Gamma_3}. \tag{35}$$

施加远场条件 $\sigma_x^\infty = \sigma_y^\infty = 0, \tau_{xy}^\infty \neq 0$ 求出平均切应力 $\bar{\sigma}_{xy}$ 和平均切应变 $\bar{\epsilon}_{xy}$ 后,可求得有效面内剪切模量:

$$\mu_4 = \frac{\bar{\sigma}_{xy}}{2\bar{\epsilon}_{xy}} = \frac{c_1(3a_3^{(1)}R_1^2 + b_1^{(1)}) + c_2[3a_3^{(2)}(R_1^2 + R_2^2) + b_1^{(2)}] + c_3[3a_3^{(3)}(R_2^2 + R_3^2) + b_1^{(3)}]}{(c_1/\mu_1)(3a_3^{(1)}R_1^2 + b_1^{(1)}) + (c_2/\mu_2)[3a_3^{(2)}(R_1^2 + R_2^2) + b_1^{(2)}] + (c_3/\mu_3)[3a_3^{(3)}(R_2^2 + R_3^2) + b_1^{(3)}]}. \quad (36)$$

上式亦为一个隐式表达式,在由式(35)求出体积模量后,需联立方程(B3)~(B6)数值求解才能确定 μ_4 .

3 算例与讨论

算例1 基于界面模型的界面效应分析

取纤维和基体的 Lamé系数分别为 $\lambda_f = 50.66$ GPa, $\mu_f = 19.0$ GPa和 $\lambda_m = 64.43$ GPa, $\mu_m = 32.9$ GPa^[26], 界面模量 $E^{S_f} = \pm 10$ N/m^[26]和 ± 5 N/m, 纤维体积分数 $c_f = 0.3$, 纤维半径 R_f 取值范围为 $1 \sim 20$ nm. 图2给出了界面模量 E^{S_f} 不同取值时无量纲有效体积模量 B_{em}/B_m 与有效面内剪切模量 μ_{em}/μ_m 随纤维半径 R_f 的变化, 其中 $E^{S_f} = 0$ N/m代表无界面效应时的结果. 由图可见, 模量存在着显著的尺度依赖性. E^{S_f} 为正时, 模量高于无界面效应时的结果; E^{S_f} 为负时, 模量低于无界面效应时的结果. 随着纤维半径的增加, 模量逐渐趋近于无界面效应时的结果. E^{S_f} 的绝对值越大, 模量与无界面效应时的结果差别越显著.

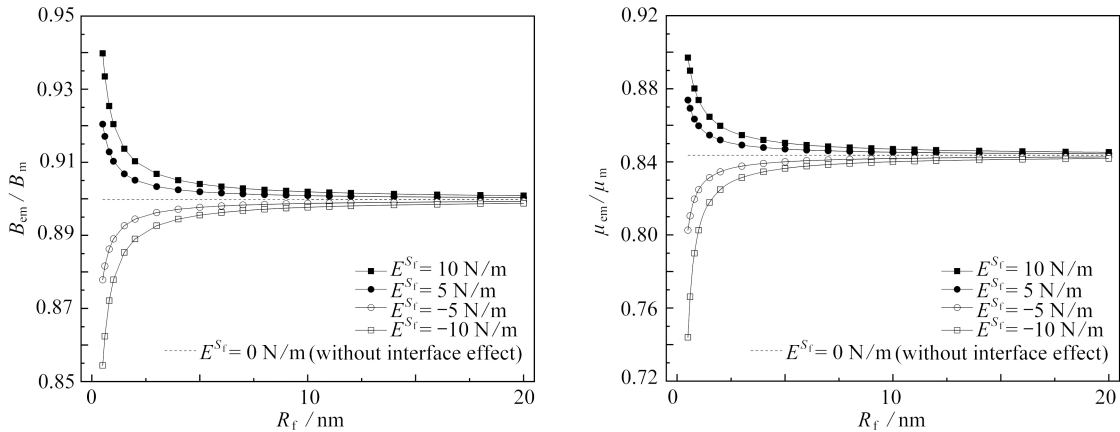


图2 无量纲有效体积模量和有效面内剪切模量随纤维半径的变化

Fig. 2 Variations of the dimensionless effective bulk modulus and the in-plane shear modulus with the fiber radius

取纤维体积分数 $c_f = 0.3$, 纤维半径 $R_f = 3$ nm, 保持基体刚度不变, 图3给出了 B_{em}/B_m 与 μ_{em}/μ_m 随纤维刚度的变化. 由图可见, 纤维刚度过大或过小结果都趋于稳定. 随着纤维刚度的减小, 模量趋近于含纳米孔洞时的结果, $E^{S_f} = 10$ N/m, 0 N/m和 -10 N/m时(代表纳米孔洞表面具有不同的界面模量)的结果存在差异. 而随着纤维刚度的增加, 界面效应逐渐减小直至消失. 进一步的计算表明, 保持纤维刚度不变而增加基体刚度, 界面效应亦逐渐减小直至消失. 总之, 界面两侧只要有一侧的材料的刚度足够大, 就可以忽略界面效应的影响.

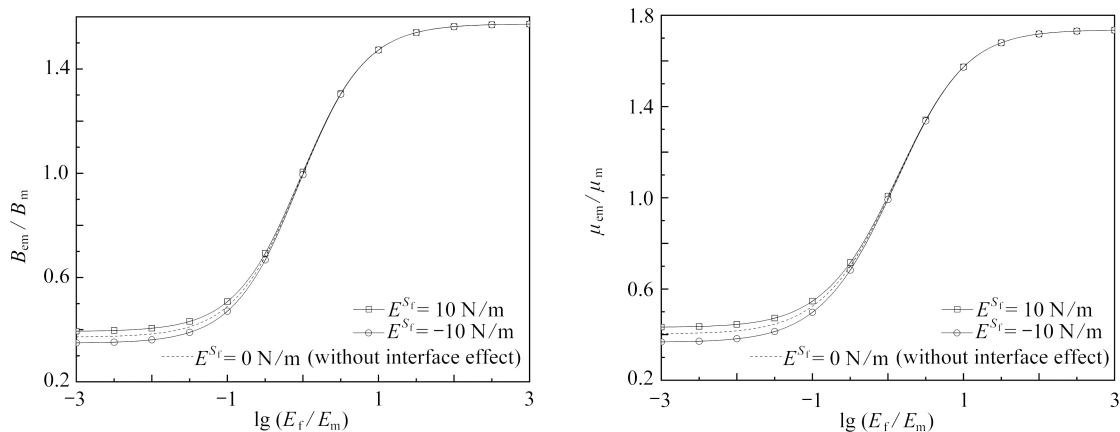


图3 无量纲有效体积模量和有效面内剪切模量随纤维刚度的变化

Fig. 3 Variations of the dimensionless effective bulk modulus and the in-plane shear modulus with the fiber rigidity

算例 2 界面相模型退化为界面模型

在讨论界面相模型模拟界面模型的问题时, Wang 等^[22] 采用的界面相性质与界面性质之间的关系为

$$\lambda_s = \frac{2\mu_1\nu_1 t}{1 - \nu_1}, \mu_s = \mu_1 t, \tag{37}$$

式中, λ_s 和 μ_s 为界面模型的界面 Lamé系数, μ_1 和 ν_1 为界面相模型中界面相的剪切模量和 Poisson 比, t 为界面相厚度。

界面模型中的界面无厚度, 其仅提供拉伸刚度. 实际上, 有限元分析中界面效应可用定义在两相界面处的杆单元模拟^[25]. 因此, 本文在用界面相模型模拟界面模型时, 取界面相 Ω_2 的 Poisson 比 $\nu_2 = 0$, 由式 (37), 界面弹性模量可表示为 $E_2 = E^{S_f}/t$, $t=R_2-R_1$ 为界面相厚度. 计算参数同算例 1, 为由界面相模型得到界面模型的结果, 令界面相厚度逐渐减小, 计算结果如表 1 所示. 由表 1 可见, 随着界面相厚度 t 的减小, 计算结果逐渐稳定并趋于界面模型的结果, 表明由界面相模型可以得到界面模型的结果. 其中由于两个模型的有效体积模量均为封闭解析解, 两者计算结果可以达到任意精度下的完全一致. 而有效面内剪切模量需要通过对隐式方程数值求解, 两者最后的稳定解有微小的差别. 事实上, 由于有效体积模量是封闭解析解, 界面模型的结果 (式 (23)) 可以由界面相模型的结果 (式 (35)) 解析退化得到, 具体证明见附录 C.

表 1 体积模量和剪切模量的退化
Table 1 Degradation of the bulk modulus and the shear modulus

$E^{S_f}/(\text{N/m})$		interphase model t/nm					interface model	
		10^{-1}	10^{-2}	10^{-3}	10^{-4}	10^{-5}		10^{-6}
10	B_{em}/B_m	0.886 87	0.906 10	0.906 77	0.906 82	0.906 83	0.906 83	0.906 83
	μ_{em}/μ_m	0.849 55	0.854 38	0.854 38	0.854 38	0.854 38	0.854 38	0.854 61
-10	B_{em}/B_m	0.900 76	0.892 14	0.892 58	0.892 64	0.892 65	0.892 65	0.892 65
	μ_{em}/μ_m	0.834 82	0.831 02	0.831 13	0.831 15	0.831 15	0.831 15	0.831 37

算例 3 界面模型与界面相模型的结果对比

为了对比界面模型与界面相模型的结果, 需已知界面与界面相力学性能参数之间的关系, 这方面的研究目前还很少见. Paliwal 等^[18] 利用能量方法并结合分子动力学模拟和 VRH 取向平均技术, 给出了含纳米孔洞金属铝孔边界面的力学性能参数 (界面模型用) 和与之对应的孔边材料过渡区的力学性能参数 (界面相模型用). 本文中考虑了两种晶格取向 (A- $\{111\}$ 取向和 B- $\{100\}$ 取向) 及两种界面相厚度 ($t_1 = 3a/2$ 和 $t_2 = 5a/2$, $a = 0.405 \text{ nm}$ 为铝的晶格常数). 两种取向的界面 Lamé系数分别为 $\lambda^{S_f} = 6.466 \text{ N/m}$, $\mu^{S_f} = -0.375 5 \text{ N/m}$ (A- $\{111\}$ 取向) 和 $\lambda^{S_f} = -2.728 5 \text{ N/m}$, $\mu^{S_f} = -6.217 8 \text{ N/m}$ (B- $\{100\}$ 取向). 由式 (16) 计算得到的界面模量 E^{S_f} 分别为 5.715 N/m (A- $\{111\}$ 取向) 和 $-15.164 1 \text{ N/m}$ (B- $\{100\}$ 取向), 对应的界面相性能参数见表 2. 铝的体积模量和剪切模量分别为 75.60 GPa 和 26.14 GPa ^[18], 孔洞体积分数为 0.3, 夹杂 (孔洞) 的体积模量和剪切模量等于 0. 假设孔洞半径变化时界面相厚度不变^[18], 本文两种模型计算结果的比较见图 4, 图中 B_0 和 μ_0 分别为无界面效应时的有效体积模量和有效面内剪切模量.

表 2 界面相力学性质^[18]
Table 2 Properties of the interphase^[18]

	A- $\{111\}$		B- $\{100\}$	
	t_1	t_2	t_1	t_2
bulk modulus B_2/GPa	80.90	79.17	74.37	75.21
shear modulus μ_2/GPa	26.75	26.61	21.19	23.46

由图 4 可见, 对界面相模型, 除了界面相 B 两种厚度的有效体积模量在孔洞半径较小时有明显差别外, 其他情况计算结果差别很小. 孔洞半径较小时, 界面模型的结果与界面相模型的结果差别明显, 且随着孔洞半径的减小差别越来越显著. 对正的界面模量 (A- $\{111\}$ 取向, $E^{S_f} = 5.715 \text{ N/m}$), 界面模型预测的有效模量高于界面相的结果, 但对负的界面模量 (B- $\{100\}$ 取向, $E^{S_f} = -15.164 1 \text{ N/m}$), 界面模型预测的有效模量低于界面相模型的结果. 随着孔洞半径的增加, 两个模型的结果相互接近, 并趋于无界面效应时的结果.

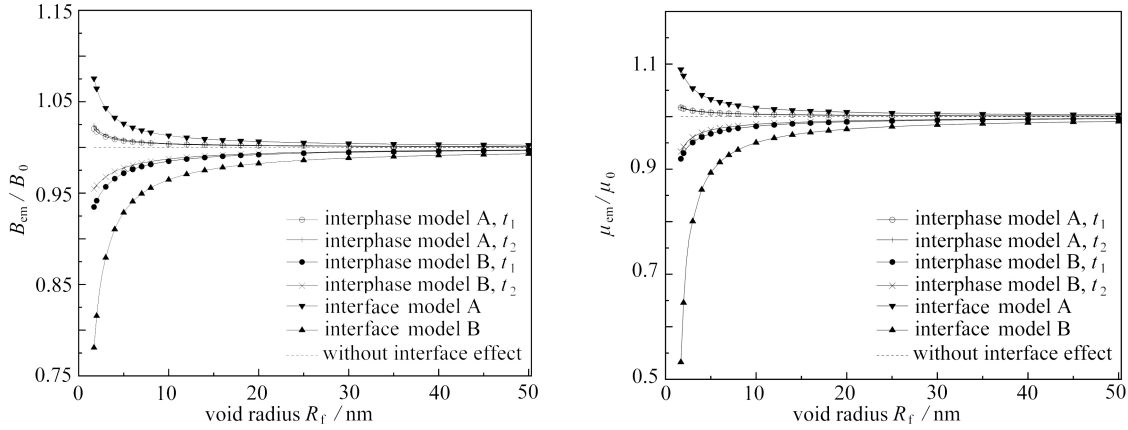


图4 界面模型和界面相模型的结果对比

Fig. 4 Results comparisons between the interface model and the interphase model

4 结 论

本文利用界面模型和界面相模型研究了纳米纤维复合材料的有效体积模量和有效面内剪切模量,给出了两种模型下有效体积模量的封闭解析解和计算有效面内剪切模量数值解的全部公式.由两个模型的解答,证明了界面相模型可以退化为界面模型,其中有效体积模量可实现解析退化,有效面内剪切模量则可以实现数值退化.由于无需处理类似于界面模型中的界面应力跳跃及由此带来的平均应力计算等复杂问题,相较于界面模型,界面相模型更便于求解.数值算例表明有效体积模量和有效面内剪切模量存在显著的尺度效应.基于界面模型的研究表明,当界面两侧有一侧的材料刚度很大时,界面效应显著减小甚至消失.当孔洞半径较小时,界面模型的结果与界面相模型的结果存在较大差异.随着孔洞半径的增加,两个模型计算结果的差异也逐渐减小.

附录 A

$$a_1^f \kappa_f R_f - \bar{a}_1^f R_f - a_1^m \kappa_m C_1 R_f + \bar{a}_1^m C_1 R_f + \bar{b}_{-1}^m C_1 / R_f = 0, \tag{A1}$$

$$a_1^m (1 - C_3) + \bar{a}_1^m (1 - C_3) + b_{-1}^m (1 + C_4) / R_f^2 - a_1^f - \bar{a}_1^f + \bar{b}_{-1}^m C_4 / R_f^2 = 0, \tag{A2}$$

$$a_1^m \kappa_m R_m - \bar{a}_1^m R_m - \bar{b}_{-1}^m / R_m - a_1^{em} C_2 \kappa_{em} R_m + \bar{a}_1^{em} C_2 R_m + \bar{b}_{-1}^{em} C_2 / R_m = 0, \tag{A3}$$

$$a_1^m R_m + \bar{a}_1^m R_m + \bar{b}_{-1}^m / R_m - a_1^{em} R_m - \bar{a}_1^{em} R_m - \bar{b}_{-1}^{em} / R_m = 0, \tag{A4}$$

$$3\bar{a}_3^f R_f^3 + \bar{b}_1^f R_f + a_{-1}^m \kappa_m C_1 / R_f - 3\bar{a}_3^m C_1 R_f^3 - \bar{b}_1^m C_1 R_f = 0, \tag{A5}$$

$$a_{-1}^m (C_3 - 2C_4 - 1) / R_f^2 + \bar{a}_3^m (1 - 3C_3 - 6C_4) R_f^2 + b_{-3}^m (1 + 3C_4) / R_f^4 - \bar{a}_3^f R_f^2 - \bar{b}_1^m C_4 = 0, \tag{A6}$$

$$a_{-1}^m \kappa_m / R_m - 3\bar{a}_3^m R_m^3 - \bar{b}_1^m R_m - a_{-1}^{em} C_2 \kappa_{em} / R_m + \bar{b}_1^{em} C_2 R_m = 0, \tag{A7}$$

$$a_{-1}^m / R_m + 3\bar{a}_3^m R_m^3 + \bar{b}_1^m R_m - a_{-1}^{em} / R_m - \bar{b}_1^{em} R_m = 0, \tag{A8}$$

$$a_3^f \kappa_f R_f^3 - a_3^m \kappa_m C_1 R_f^3 - \bar{a}_{-1}^m C_1 / R_f + \bar{b}_{-3}^m C_1 / R_f^3 = 0, \tag{A9}$$

$$3\bar{a}_3^m (C_3 + 2C_4 - 1) R_f^2 + \bar{a}_{-1}^m (2C_4 - C_3 - 1) / R_f^2 + (C_4 - 1) b_1^m + 3\bar{a}_3^f R_f^2 + \bar{b}_1^f - 3\bar{b}_{-3}^m C_4 / R_f^4 = 0, \tag{A10}$$

$$a_3^m \kappa_m R_m^3 + \bar{a}_{-1}^m / R_m - \bar{b}_{-3}^m / R_m^3 - a_{-1}^{em} C_2 / R_m + \bar{b}_{-3}^{em} C_2 / R_m^3 = 0, \tag{A11}$$

$$a_3^m R_m^3 - \bar{a}_{-1}^m / R_m + \bar{b}_{-3}^m / R_m^3 + a_{-1}^{em} / R_m - \bar{b}_{-3}^{em} / R_m^3 = 0, \tag{A12}$$

式中, $C_1 = \mu_f / \mu_m$, $C_2 = \mu_m / \mu_{em}$, $C_3 = E^{Sf} / (2\Gamma_m R_f)$, $C_4 = E^{Sf} / (4\mu_m R_f)$.

附录 B

$$a_1^{(i)} \kappa_i R_i - \bar{a}_1^{(i)} R_i - \bar{b}_{-1}^{(i)} / R_i - a_1^{(i+1)} g_{i(i+1)} \kappa_{i+1} R_i + \bar{a}_1^{(i+1)} g_{i(i+1)} R_i + \bar{b}_{-1}^{(i+1)} g_{i(i+1)} / R_i = 0, \tag{B1}$$

$$a_1^{(i)} R_i + \bar{a}_1^{(i)} R_i + \bar{b}_{-1}^{(i)} / R_i - a_1^{(i+1)} R_i - \bar{a}_1^{(i+1)} R_i - \bar{b}_{-1}^{(i+1)} / R_i = 0, \tag{B2}$$

$$a_{-1}^{(i)}\kappa_i/R_i - 3\overline{a_3^{(i)}}R_i^3 - \overline{b_1^{(i)}}R_i - a_{-1}^{(i+1)}g_{i(i+1)\kappa_{i+1}}/R_i + 3\overline{a_3^{(i+1)}}g_{i(i+1)}R_i^3 + \overline{b_1^{(i+1)}}g_{i(i+1)}R_i = 0, \tag{B3}$$

$$a_{-1}^{(i)}/R_i + 3\overline{a_3^{(i)}}R_i^3 + \overline{b_1^{(i)}}R_i - a_{-1}^{(i+1)}/R_i - 3\overline{a_3^{(i+1)}}R_i^3 - \overline{b_1^{(i+1)}}R_i = 0, \tag{B4}$$

$$a_3^{(i)}\kappa_i R_i^3 + \overline{a_{-1}^{(i)}}/R_i - \overline{b_{-3}^{(i)}}/R_i^3 - a_3^{(i+1)}g_{i(i+1)\kappa_{i+1}}R_i^3 - \overline{a_{-1}^{(i+1)}}g_{i(i+1)}/R_i + \overline{b_{-3}^{(i+1)}}g_{i(i+1)}/R_i^3 = 0, \tag{B5}$$

$$a_3^{(i)}R_i^3 - \overline{a_{-1}^{(i)}}/R_i + \overline{b_{-3}^{(i)}}/R_i^3 - a_3^{(i+1)}R_i^3 + \overline{a_{-1}^{(i+1)}}/R_i - \overline{b_{-3}^{(i+1)}}/R_i^3 = 0, \tag{B6}$$

式中, $g_{i(i+1)} = \mu_i/\mu_{i+1}$, $a_{-1}^{(1)} = a_3^{(4)} = b_{-1}^{(1)} = b_{-3}^{(1)} = 0$, $i=1, 2, 3$.

附录 C

在界面相模型中取界面相 Ω_2 的 Poisson 比 $\nu_2 = 0$, 弹性模量 $E_2 = \lim_{t \rightarrow 0} \frac{E^{Sf}}{t}$, $t=R_2-R_1$ 为界面相厚度. 当界面相厚度趋近于 0 时, 界面相 Ω_2 的体积分数 $c_2 = 0$. 在此情况下, 两个模型中符号的对应关系如表 C1 所示.

表 C1 界面模型和界面相模型中的对应符号

Table C1 Corresponding symbols in the interface model and the interphase model

interphase model	interface model
R_1, R_3	R_f, R_m
c_1, c_3	c_f, c_m
Γ_1, Γ_3	Γ_f, Γ_m
$\Omega_1, \Omega_3, \Omega_4$	$\Omega_f, \Omega_m, \Omega_{em}$

在式 (35) 中

$$L_2 = \frac{(2g_{23} + \kappa_2 - 1)(2g_{12} + \kappa_1 - 1) + 2\left(\frac{R_1}{R_2}\right)^2 (g_{23} - 1)[g_{12}(\kappa_2 - 1) - \kappa_1 + 1]}{g_{12}g_{23}(\kappa_2 + 1)(\kappa_3 + 1)} =$$

$$\frac{\left(\frac{\mu_2}{\mu_3} + 1 - 2\nu_2\right)\left(\frac{\mu_1}{\mu_2} + 1 - 2\nu_1\right) + \left(\frac{R_1}{R_2}\right)^2 \left(\frac{\mu_2}{\mu_3} - 1\right)\left[\frac{\mu_1}{\mu_2}(1 - 2\nu_2) - (1 - 2\nu_1)\right]}{4\frac{\mu_1}{\mu_3}(1 - \nu_2)(1 - \nu_3)} =$$

$$\frac{\left(\frac{\mu_2}{\mu_3} + 1\right)\left(\frac{\mu_1}{\mu_2} + 1 - 2\nu_1\right) + \left(\frac{R_1}{R_2}\right)^2 \left(\frac{\mu_2}{\mu_3} - 1\right)\left[\frac{\mu_1}{\mu_2} - (1 - 2\nu_1)\right]}{4\frac{\mu_1}{\mu_3}(1 - \nu_3)} =$$

$$\frac{\frac{\mu_1}{\mu_3} + \frac{\mu_2}{\mu_3}(1 - 2\nu_1) + \frac{\mu_1}{\mu_2} + (1 - 2\nu_1) + \left(\frac{R_1}{R_2}\right)^2 \frac{\mu_1}{\mu_3} - \left(\frac{R_1}{R_2}\right)^2 \frac{\mu_2}{\mu_3}(1 - 2\nu_1) - \left(\frac{R_1}{R_2}\right)^2 \frac{\mu_1}{\mu_2} + \left(\frac{R_1}{R_2}\right)^2 (1 - 2\nu_1)}{4\frac{\mu_1}{\mu_3}(1 - \nu_3)} =$$

$$\frac{\frac{\mu_1}{\mu_3}\left(1 + \frac{R_1^2}{R_2^2}\right) + \frac{\mu_2}{\mu_3}(1 - 2\nu_1)\left(1 - \frac{R_1^2}{R_2^2}\right) + \frac{\mu_1}{\mu_2}\left(1 - \frac{R_1^2}{R_2^2}\right) + (1 - 2\nu_1)\left(1 + \frac{R_1^2}{R_2^2}\right)}{4\frac{\mu_1}{\mu_3}(1 - \nu_3)} =$$

$$\frac{2\frac{\mu_f}{\mu_m} + \frac{E^{Sf}(1 + \nu_m)(1 - 2\nu_f)}{(R_2 - R_1)E_m}\left(\frac{R_2^2 - R_1^2}{R_2^2}\right) + 2(1 - 2\nu_f)}{4\frac{\mu_f}{\mu_m}(1 - \nu_m)} = \frac{2\frac{\mu_f}{\mu_m} + 2\frac{E^{Sf}(1 + \nu_m)}{R_f E_m}(1 - 2\nu_f) + 2(1 - 2\nu_f)}{4\frac{\mu_f}{\mu_m}(1 - \nu_m)} =$$

$$\frac{2\frac{\mu_f}{\mu_m} + \frac{E^{Sf}(1 + \nu_m)}{R_f E_m}(2 - 4\nu_f) + (2 - 4\nu_f)}{\frac{\mu_f}{\mu_m}(4 - 4\nu_m)} = \frac{2\frac{\mu_f}{\mu_m} + \frac{E^{Sf}}{2\mu_m R_f}(3 - 4\nu_f - 1) + (3 - 4\nu_f - 1)}{\frac{\mu_f}{\mu_m}(3 - 4\nu_m + 1)} =$$

$$\frac{2C_1 + 2C_4(\kappa_f - 1) + (\kappa_f - 1)}{C_1(\kappa_m + 1)} = \frac{2C_1 + (2C_4 + 1)(\kappa_f - 1)}{C_1(\kappa_m + 1)} = M_1, \tag{C1}$$

$$L_1 c_2 = \frac{2g_{12} + \kappa_1 - 1}{812(\kappa_2 + 1)} \frac{R_2^2 - R_1^2}{R_3^2} = \frac{\frac{\mu_1}{\mu_2} + 1 - 2\nu_1}{2} \frac{R_2^2 - R_1^2}{R_3^2} = \frac{(R_2 - R_1)E_1}{E^{S_f}(1 + \nu_1)} + 1 - 2\nu_1 \frac{R_2^2 - R_1^2}{R_3^2} =$$

$$\frac{(R_2 - R_1)E_1 + E^{S_f}(1 + \nu_1)(1 - 2\nu_1)}{E^{S_f}(1 + \nu_1)} \frac{E^{S_f}(1 + \nu_1)}{2(R_2 - R_1)E_1} \frac{R_2^2 - R_1^2}{R_3^2} =$$

$$\frac{E^{S_f}(1 + \nu_f)(1 - 2\nu_f)R_f}{E_f R_m^2}, \quad (C2)$$

$$\frac{L_1 c_2}{\Gamma_2} = \frac{E^{S_f}(1 + \nu_f)(1 - 2\nu_f)R_f}{\Gamma_2 E_f R_m^2} = \frac{2E^{S_f}(1 + \nu_f)^2(1 - 2\nu_f)^2 R_f}{E_2 E_f R_m^2} =$$

$$\frac{2E^{S_f}(1 + \nu_f)^2(1 - 2\nu_f)^2 R_f(R_2 - R_1)}{E^{S_f} E_f R_m^2} = 0. \quad (C3)$$

在式(23)中

$$M_1 C_3 c_f - \frac{M_{-1} C_4 c_f}{R_f^2} = \frac{(2C_4 + 1)(\kappa_f - 1) + 2C_1}{C_1(\kappa_m + 1)} C_3 c_f - \frac{2R_f^2 [(C_3 - 1)(\kappa_f - 1) + C_1(\kappa_m - 1)]}{C_1(\kappa_m + 1)R_f^2} C_4 c_f =$$

$$\frac{\left\{ \left[\frac{E^{S_f}(1 + \nu_m)}{R_f E_m} + 1 \right] (2 - 4\nu_f) + 2 \frac{\mu_f}{\mu_m} \right\} E^{S_f}(1 + \nu_m)(1 - 2\nu_m)}{\frac{\mu_f}{\mu_m} (3 - 4\nu_m + 1) R_f E_m} c_f -$$

$$\frac{\left\{ \left[\frac{E^{S_f}(1 + \nu_m)(1 - 2\nu_m)}{R_f E_m} - 1 \right] (2 - 4\nu_f) + \frac{\mu_f}{\mu_m} (2 - 4\nu_m) \right\} E^{S_f}(1 + \nu_m)}{\frac{\mu_f}{\mu_m} (3 - 4\nu_m + 1) R_f E_m} c_f =$$

$$\frac{(2 - 4\nu_f) E^{S_f}(1 + \nu_m)(2 - 2\nu_m)}{E_f(1 + \nu_m)(3 - 4\nu_m + 1) R_f E_m} \frac{R_f^2}{R_m^2} =$$

$$\frac{E^{S_f}(1 + \nu_f)(1 - 2\nu_f)R_f}{E_f R_m^2}. \quad (C4)$$

由式(C2)和式(C4)可知

$$L_1 c_2 = M_1 C_3 c_f - \frac{M_{-1} C_4 c_f}{R_f^2}. \quad (C5)$$

将式(C1)、(C3)和(C5)代入式(35),可得

$$B_4 = \frac{c_f + M_1(1 - c_f) + M_1 C_3 c_f - \frac{M_{-1} C_4 c_f}{R_f^2}}{\frac{c_f}{\Gamma_f} + \frac{M_1(1 - c_f)}{\Gamma_m}} = B_{em}, \quad (C6)$$

即界面相模型的有效体积模量(式(35))解析退化为界面模型的有效体积模量(式(23)).

参考文献(References):

- [1] 刘旭, 姚林泉. 热环境中旋转功能梯度纳米环板的振动分析[J]. 应用数学和力学, 2020, 41(11): 1224-1236. (LIU Xu, YAO Linquan. Vibration analysis of rotating functionally gradient nano annular plates in thermal environment[J]. *Applied Mathematics and Mechanics*, 2020, 41(11): 1224-1236.(in Chinese))
- [2] SHUKLA P, SAXENA P. Polymer nanocomposites in sensor applications: a review on present trends and future scope[J]. *Chinese Journal of Polymer Science*, 2021, 39(6): 665-691.
- [3] CAMMARATA R C. Surface and interface stress effects on interfacial and nanostructured materials[J]. *Materials Science and Engineering: A*, 1997, 237(2): 180-184.
- [4] 周强, 张志纯, 龙志林, 等. 考虑表面效应的压电纳米梁的振动研究[J]. 应用数学和力学, 2020, 41(8): 853-865. (ZHOU Qiang, ZHANG Zhichun, LONG Zhilin, et al. Vibration of piezoelectric nanobeams with surface effects[J]. *Applied Mathematics and Mechanics*, 2020, 41(8): 853-865.(in Chinese))
- [5] GURTIN M E, MURDOCH A I. A continuum theory of elastic material surfaces[J]. *Archive for Rational Mech-*

- anics and Analysis*, 1975, **57**(4): 291-323.
- [6] GURTIN M E, MURDOCH A I. Surface stress in solids[J]. *International Journal of Solids and Structures*, 1978, **14**(6): 431-440.
- [7] ODEGARD G M, CLANCY T C, GATES T S. Modeling of the mechanical properties of nanoparticle/polymer composites[J]. *Polymer*, 2005, **46**(2): 553-562.
- [8] PALIWAL B, CHERKAOUI M. Estimation of anisotropic elastic properties of nanocomposites using atomistic-continuum interphase model[J]. *International Journal of Solids and Structures*, 2012, **49**(18): 2424-2438.
- [9] LUO J, WANG X. On the anti-plane shear of an elliptic nano inhomogeneity[J]. *European Journal of Mechanics A: Solids*, 2009, **28**(5): 926-934.
- [10] TIAN L, RAJAPAKSE R K N D. Analytical solution for size-dependent elastic field of a nanoscale circular inhomogeneity[J]. *Journal of Applied Mechanics*, 2007, **74**(3): 568-574.
- [11] TIAN L, RAJAPAKSE R K N D. Elastic field of an isotropic matrix with a nanoscale elliptical inhomogeneity[J]. *International Journal of Solids and Structures*, 2007, **44**(24): 7988-8005.
- [12] DONG C Y, PAN E. Boundary element analysis of nano-inhomogeneities of arbitrary shapes with surface and interface effects[J]. *Engineering Analysis With Boundary Elements*, 2011, **35**(8): 996-1002.
- [13] MOGILEVSKAYA S G, CROUCH S L, STOLARSKI H K. Multiple interacting circular nano-inhomogeneities with surface/interface effects[J]. *Journal of the Mechanics and Physics of Solids*, 2008, **56**(6): 2298-2327.
- [14] DUAN H L, WANG J, HUANG Z P. Size-dependent effective elastic constants of solids containing nano-inhomogeneities with interface stress[J]. *Journal of the Mechanics and Physics of Solids*, 2005, **53**(7): 1574-1596.
- [15] CHEN T Y, DVORAK G J, YU C C. Solids containing spherical nano-inclusions with interface stresses: effective properties and thermal-mechanical connections[J]. *International Journal of Solids and Structures*, 2007, **44**(3/4): 941-955.
- [16] 肖俊华, 徐耀玲, 王美芬, 等. 考虑界面应力时纳米涂层纤维增强复合材料的有效力学性能[J]. *固体力学学报*, 2013, **34**(4): 374-379. (XIAO Junhua, XU Yaoling, WANG Meifen, et al. Effective mechanical property of nano coated fiber reinforced composites due to interface stress[J]. *Chinese Journal of Solid Mechanics*, 2013, **34**(4): 374-379.(in Chinese))
- [17] LI Y, WAAS A M, ARRUDA A E. A closed-form, hierarchical, multi-interphase model for composites-derivation, verification and application to nanocomposites[J]. *Journal of the Mechanics and Physics of Solids*, 2011, **59**(1): 43-63.
- [18] PALIWAL B, CHERKAOUI M. Atomistic-continuum interphase model for effective properties of composite materials containing nano-inhomogeneities[J]. *Philosophical Magazine*, 2011, **91**(30): 3905-3930.
- [19] WANG Z, OELKERS R J, LEE K C, et al. Annular coated inclusion model and applications for polymer nanocomposites, part I: spherical inclusions[J]. *Mechanics of Materials*, 2016, **101**: 170-184.
- [20] WANG Z, OELKERS R J, LEE K C, et al. Annular coated inclusion model and applications for polymer nanocomposites, part II: cylindrical inclusions[J]. *Mechanics of Materials*, 2016, **101**: 50-60.
- [21] BENVENISTE Y, MILOH T. Imperfect soft and stiff interfaces in two-dimensional elasticity[J]. *Mechanics of Materials*, 2001, **33**(6): 309-323.
- [22] WANG J, DUAN H L, ZHANG Z. An anti-interpenetration model and connections between interphase and interface models in particle-reinforced composites[J]. *International Journal of Mechanical Sciences*, 2005, **47**(4/5): 701-718.
- [23] MUSKHELISHVILI N I. *Some Basic Problem of the Mathematical Theory of Elasticity*[M]. Leyden: Noordhoff International Publishing, 1977.
- [24] PARVANOV S L, VASILEV G P, DINEVA P S, et al. Dynamic analysis of nano-heterogeneities in a finite-size solid by boundary and finite element methods[J]. *International Journal of Solids and Structures*, 2016, **80**(1): 1-18.
- [25] WANG W F, ZENG X W, DING J P. Finite element modeling of two-dimensional nanoscale structures with surface effects[J]. *World Academy of Science, Engineering and Technology*, 2010, **48**: 865-870.
- [26] TIAN L, RAJAPAKSE R K N D. Finite element modelling of nanoscale inhomogeneities in an elastic matrix[J]. *Computational Materials Science*, 2004, **41**(1): 44-53.